Spatial Modulation in the Presence of I/Q Imbalance: Optimal Detector & Performance Analysis

Ayse E. Canbilen, Malek M. Alsmadi, Ertugrul Basar, *Senior Member, IEEE*, Salama S. Ikki, *Member, IEEE*, Seyfettin S. Gultekin, and Ibrahim Develi

***Abstract*— Spatial modulation (SM) is affected by the impacts of in-phase and quadrature-phase imbalance (IQI), which cause degradation of system performance in practical terms. To address this concern, an optimal maximum likelihood detector is proposed for SM-based transmission and the system performance is analyzed by computer simulations and analytical derivations. In addition, this optimal receiver is compared with a non-optimal receiver. Specifically, pairwise and average bit error probabilities are derived for the optimal detector. The results prove that IQI is a critical issue for SM-based transmission and the proposed optimal receiver significantly enhances the SM system performance in the presence of IQI.**

***Index Terms*— Error performance analysis, I/Q imbalance, maximum likelihood detection, spatial modulation.**

I. Introduction

MULTIPLE-INPUT multiple-output (MIMO) systems, which often utilize the direct conversion architecture (DCA) to ensure low power implementation, will play a key role in next-generation wireless networks [1]–[2]. The undesirable input signal, called image, is rejected by signal processing in in-phase (I) and quadrature-phase (Q) arms instead of external filters in DCA [2]. Although DCA theoretically provides infinite attenuation of the image band by using quadrature mixing, in practice, it suffers from several major analog radio frequency (RF) impairments based on physical constraints.

One of these imperfections is the I/Q imbalance (IQI), which is caused by the mismatch between the I and Q components from the ideal case (i.e., equal amplitudes and 90° phase difference). The main reason for this critical issue is the limited tolerance of the capacitors and resistors used in analog RF elements. IQI not only induces crosstalk, power loss, and frequency interference, but also results in performance degradation. Additionally, IQI has more deterioration effects on systems that have high data rates and use high order modulation techniques [3]. Hence, the evaluation of the impacts of IQI is crucial for the design of next-generation communication systems [4].

Spatial modulation (SM) was proposed to solve the most of the inherent MIMO system drawbacks [5]. In SM, just one of the transmit antennas (TAs) is activated, and the others are kept inactive during each transmission time. Therefore, the need for TAs synchronization as well as inter-channel interference at the receiver (Rx) is completely removed [5]. The index of the activated antenna is used as extra information to achieve spatial gain [6]. Consequently, it increases both the energy efficiency (EE) and the spectral efficiency (SE) at the same time [7].

The effect of IQI on SM-based MIMO transmission was discussed in only two letters in previous literature [8], [9]. Firstly, it was observed that both amplitude and phase IQI cause significant performance degradation for SM-based transmission [8]. However, the authors did not propose an optimal solution for the IQI effect. Secondly, the transmitter (Tx) IQI sensitivity of SM was investigated in [9]. Nevertheless, as some of the information bits are transmitted with the active antenna indices, both Tx and Rx IQI have destructive effects on the Rx detection procedure [9]. As a result, the consideration of the IQI effect only at Tx side is not enough to interpret this impairment for SM [10].

In this letter, an optimal Rx is designed for the SM scheme operating in the presence of IQI effect on the Rx side and the error performance is evaluated via computer simulations and analytical derivations. This novel Rx design is superior to the existing ones since it not only obtains the optimal performance results but can also be easily expanded into a form, which includes Tx IQI imperfections. To the best of the authors' knowledge, such design does not exist in the current literature.

Notation: Bold lower and upper case letters denote vectors and matrices, respectively. $\mathcal{CN}(\mu, \sigma_n^2)$ represents the complex Gaussian distribution with mean μ and variance σ_n^2. $(\cdot)^I$ and $(\cdot)^Q$ denote the I and Q parts, respectively. a_j denotes the j^{th} element of any column vector $\boldsymbol{a}$. $(\cdot)^*$ is the complex conjugate value, $\mathrm{cov}(x, y)$ is the covariance of the variables x and y, $(\cdot)^T$ is the matrix transpose and $\mathrm{E}\{\cdot\}$ denotes the expectation.

II. System and Channel Models

The SM-MIMO synchrodyne architecture transceiver model, which is used in this study, is given in Fig. 1. The incoming data bit stream $\boldsymbol{q}$ is divided into blocks containing $m = \log_2(N_t M)$ bits each (M is modulation order of complex constellations and N_t is the number of TAs). These blocks are

Manuscript received March 12, 2018; revised April 21, 2018; accepted May 1, 2018. Date of publication May 15, 2018; date of current version August 10, 2018. The work of A. E. Canbilen was supported in part by The Scientific and Technological Research Council of Turkey (TUBITAK) BIDEB-2214 International Doctoral Research Fellowship Programme. The work of E. Basar was supported by Turkish Academy of Sciences (TUBA) Outstanding Young Scientist Award Programme (GEBIP). The associate editor coordinating the review of this paper and approving it for publication was Y. Xiao. *(Corresponding author: Ayse E. Canbilen.)*

A. E. Canbilen is with the Department of Electrical Engineering, Lakehead University, Thunder Bay, P7B 5E1, Canada, and also with the Electrical and Electronics Engineering Department, Selçuk University, 42130 Konya, Turkey (e-mail: acanbile@lakehedu.ca).

M. M. Alsmadi and S. S. Ikki are with the Department of Electrical Engineering, Lakehead University, Thunder Bay, P7B 5E1, Canada (e-mail: malsamdi@lakehedu.ca; sikki@lakehedu.ca).

E. Basar is with the Faculty of Electrical and Electronics Engineering, Istanbul Technical University, 34469 Istanbul, Turkey (e-mail: basarer@itu.edu.tr).

S. S. Gultekin is with the Electrical and Electronics Engineering Department, Selçuk University, 42130 Konya, Turkey (e-mail: sgultekin@selcuk.edu.tr).

I. Develi is with the Electrical and Electronics Engineering Department, Erciyes University, 38039 Kayseri, Turkey (e-mail: develi@erciyes.edu.tr).

Digital Object Identifier 10.1109/LCOMM.2018.2836448

further partitioned into two sub-blocks to identify the spatial and the quadrature amplitude modulation (QAM) bits at Tx side. Spatial bits determine a Tx antenna (TA) to switch on for transmission and SM demultiplexer block assigns the signal to the activated TA. The signal vector $\boldsymbol{u}$ passes through an $N_r \times N_t$ sized channel $\boldsymbol{H}$ (N_r is the number of Rx antennas), whose columns represent the complex fading gain coefficients between the i^{th} TA and the Rx antennas as vectors, i.e., $\boldsymbol{h}_i = \boldsymbol{h}_i^I + j\boldsymbol{h}_i^Q$ $(i = 1, ..., N_t)$. The entries of $\boldsymbol{h}_i$ are assumed to follow $\mathcal{CN}(0,1)$ distribution. The transmitted signal also experiences additive white Gaussian noise, $\boldsymbol{n} = \boldsymbol{n}^I + j\boldsymbol{n}^Q \sim \mathcal{CN}(0, \sigma_n^2)$ which has independent and identical I and Q parts.

The incoming signal to the Rx antenna is first amplified by a low-noise amplifier (LNA), and quadrature mixing is applied by two local oscillator (LO) signals. IQI is introduced during this step of down-conversion, owing to the imperfect LOs. Afterward, the signal on each branch is passed through a low pass filter (LPF) and an analog to digital converter (ADC), respectively. Then, I and Q parts of the baseband signal are combined. The received signal, y_j, at Rx antenna j in the presence of IQI can be written as follows $(j = [1, ..., N_r];\ q \in \{1, ..., M\})$

$$y_j = K_1\left(\sqrt{E_u}\,(h_{ij}x_q) + n_j\right) + K_2\left(\sqrt{E_u}\,(h_{ij}x_q) + n_j\right)^*, \quad (1)$$

where h_{ij} is the corresponding channel coefficient, E_u and x_q are the transmitted signal energy and the transmitted symbol, respectively. On the other hand, Rx side IQI coefficients K_1 and K_2 are equal to [3]

$$K_1 = \frac{1}{2}\left(1 + \xi_r e^{-j\beta_r}\right), \quad K_2 = \frac{1}{2}\left(1 - \xi_r e^{j\beta_r}\right). \quad (2)$$

Here ξ_r and β_r are Rx amplitude and phase mismatches, respectively. (Note that if there is ideal matching, then $\xi_r = 1$ and $\beta_r = 0$). Defining $K_C = K_1^Q + K_2^Q$ and $K_D = K_1^I - K_2^I$, y_j is given as follows

$$\begin{aligned} y_j = \sqrt{E_u}\Big\{ & h_{ij}^I {x_q}^I - h_{ij}^Q {x_q}^Q + j\left[h_{ij}^I(x_q^I K_C + x_q^Q K_D)\right. \\ & \left. + h_{ij}^Q(x_q^I K_D - x_q^Q K_C)\right]\Big\} + n_j^I + j(n_j^I K_C + n_j^Q K_D). \end{aligned} \quad (3)$$

It can be stated that y_j has correlated I/Q components, since $\text{cov}(y_j^I, y_j^Q) = \text{E}\{y_j^I y_j^Q\} - \text{E}\{y_j^I\}\text{E}\{y_j^Q\} \neq 0$. The correlation coefficient can be calculated as

$$\varrho = \frac{\text{cov}(y_j^I, y_j^Q)}{\sigma_{y_j^I}\sigma_{y_j^Q}} = \frac{\frac{\sigma_n^2}{2}K_C}{\sqrt{\frac{\sigma_n^2}{2}\frac{\sigma_n^2}{2}\xi_r^2}} = -\sin\beta_r. \quad (4)$$

Incidentally,

$$\boldsymbol{\chi}_p^I = (\boldsymbol{h}_i^I {x_q}^I - \boldsymbol{h}_i^Q {x_q}^Q) \quad (p \in \{1, ..., N_t M\}), \quad (5)$$

$$\boldsymbol{\chi}_p^Q = \boldsymbol{h}_i^I(x_q^I K_C + x_q^Q K_D) + \boldsymbol{h}_i^Q(x_q^I K_D - x_q^Q K_C), \quad (6)$$

$$\tilde{\boldsymbol{n}}^I = \boldsymbol{n}^I, \quad \tilde{\boldsymbol{n}}^Q = \boldsymbol{n}^I K_C + \boldsymbol{n}^Q K_D. \quad (7)$$

Accordingly, stating that $\boldsymbol{\chi}_p = \boldsymbol{\chi}_p^I + j\boldsymbol{\chi}_p^Q$ and $\tilde{\boldsymbol{n}} = \tilde{\boldsymbol{n}}^I + j\tilde{\boldsymbol{n}}^Q$, (3) can be rewritten as follows

$$\boldsymbol{y} = \sqrt{E_u}\boldsymbol{\chi}_p + \tilde{\boldsymbol{n}}. \quad (8)$$

Following these operations, SM detector recovers the whole information block (activated antenna index and the transmitted symbol) by solving $c = N_t M$ hypotheses.

III. Performance Analysis

A. Optimal ML Detector

It is observed from (8) that $\boldsymbol{y}$ has correlated components and is corrupted by a zero-mean complex correlated improper Gaussian noise vector. Regarding to this, the joint probability density function (PDF) of the received signals at the Rx side is given by

$$\begin{aligned} f_{\boldsymbol{y}^I,\boldsymbol{y}^Q}(\boldsymbol{y}^I, \boldsymbol{y}^Q | \boldsymbol{\chi}_p) = & \left(\frac{1}{2\pi\sigma_{\tilde{n}_j^I}\sigma_{\tilde{n}_j^Q}\sqrt{1-\varrho^2}}\right)^{N_r} \\ & \times \exp\left(\frac{-1}{2(1-\varrho^2)}\left[\frac{\|\boldsymbol{y}^I - \sqrt{E_u}\boldsymbol{\chi}_p^I\|^2}{\sigma_{\tilde{n}_j^I}^2} + \frac{\|\boldsymbol{y}^Q - \sqrt{E_u}\boldsymbol{\chi}_p^Q\|^2}{\sigma_{\tilde{n}_j^Q}^2}\right.\right. \\ & \left.\left. - \frac{2\varrho(\boldsymbol{y}^I - \sqrt{E_u}\boldsymbol{\chi}_p^I)^T(\boldsymbol{y}^Q - \sqrt{E_u}\boldsymbol{\chi}_p^Q)}{\sigma_{\tilde{n}_j^I}\sigma_{\tilde{n}_j^Q}}\right]\right). \end{aligned} \quad (9)$$

Assuming that Rx has the perfect channel state information and channel inputs are equiprobable, optimal maximum likelihood (ML) detector for SM-MIMO system is designed by using (8) and (9) as follows ($\sigma_{\tilde{n}_j^I}^2 = \sigma_n^2/2$ and $\sigma_{\tilde{n}_j^Q}^2 = \xi_r^2\sigma_{\tilde{n}_j^I}^2$)

$$\hat{p} = \arg\min_p \left\{ \begin{array}{l} \|\boldsymbol{y}^I - \sqrt{E_u}\boldsymbol{\chi}_p^I\|^2 + \frac{1}{\xi_r^2}\|\boldsymbol{y}^Q - \sqrt{E_u}\boldsymbol{\chi}_p^Q\|^2 \\ -\frac{2\varrho}{|\xi_r|}(\boldsymbol{y}^I - \sqrt{E_u}\boldsymbol{\chi}_p^I)^T(\boldsymbol{y}^Q - \sqrt{E_u}\boldsymbol{\chi}_p^Q) \end{array} \right\}, \quad (10)$$

which jointly accounts for TA index and symbol errors. The conditional pairwise error probability (PEP) can be calculated with this decision rule assuming $\boldsymbol{\chi}_p$ is transmitted from Tx; however, erroneously $\hat{\boldsymbol{\chi}}_p$ is detected at Rx by using

$$\begin{aligned} \text{PEP}_{op} = \Pr\Bigg\{ & \frac{\|\boldsymbol{y}^I - \sqrt{E_u}\boldsymbol{\chi}_p^I\|^2}{\frac{\sigma_n^2}{2}} + \frac{\|\boldsymbol{y}^Q - \sqrt{E_u}\boldsymbol{\chi}_p^Q\|^2}{\frac{\sigma_n^2}{2}\xi_r^2} \\ & - \frac{2\varrho\left(\boldsymbol{y}^I - \sqrt{E_u}\boldsymbol{\chi}_p^I\right)^T(\boldsymbol{y}^Q - \sqrt{E_u}\boldsymbol{\chi}_p^Q)}{\frac{\sigma_n^2}{2}|\xi_r|} \\ & > \frac{\|\boldsymbol{y}^I - \sqrt{E_u}\hat{\boldsymbol{\chi}}_p^I\|^2}{\frac{\sigma_n^2}{2}} + \frac{\|\boldsymbol{y}^Q - \sqrt{E_u}\hat{\boldsymbol{\chi}}_p^Q\|^2}{\frac{\sigma_n^2}{2}\xi_r^2} \\ & - \frac{2\varrho(\boldsymbol{y}^I - \sqrt{E_u}\hat{\boldsymbol{\chi}}_p^I)^T(\boldsymbol{y}^Q - \sqrt{E_u}\hat{\boldsymbol{\chi}}_p^Q)}{\frac{\sigma_n^2}{2}|\xi_r|}\Bigg\}. \end{aligned} \quad (11)$$

The conditional PEP can also be written as in (12) by using the Q-function. However, it is not easy to find the PDF of γ, which is necessary to calculate the average PEP (APEP), in (12). Thus, the moment generating function (MGF) as an alternative representation of the Q-function of γ is utilized. Noting that γ is a quadratic form of Gaussian random variables, the required MGF is calculated as

$$M_\gamma(t) = \left(\frac{1}{\sqrt{1-2tA_1}} \times \frac{1}{\sqrt{1-2tA_2}}\right)^{N_r}. \quad (13)$$

Using (12), A_1 and A_2 in (13) can be obtained from

$$A_{1,2} = \frac{\lambda_1}{2} + \frac{\lambda_2}{2\xi_r^2} \pm \sqrt{\left(\frac{\lambda_1}{2} + \frac{\lambda_2}{2\xi_r^2}\right)^2 - \frac{(1-\varrho^2)\lambda_1\lambda_2}{\xi_r^2}}. \quad (14)$$

Here, λ_1 and λ_2 are calculated by utilizing the following expressions, where $\hat{x}_q$ and $\hat{i}$ represent the detected versions of the transmitted complex symbol and the TA index,

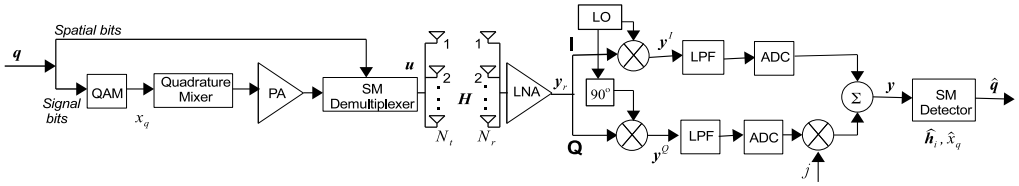

Fig. 1. System model of SM-MIMO in the presence of IQI.

respectively,

$$\lambda_1 = \begin{cases} \left[|x_q^I - \hat{x}_q^I|^2 + |x_q^Q - \hat{x}_q^Q|^2\right]/2 & (i = \hat{i}) \\ \left[|x_q^I|^2 + |\hat{x}_q^I|^2 + |x_q^Q|^2 + |\hat{x}_q^Q|^2\right]/2 & (i \neq \hat{i}). \end{cases}$$

$$\lambda_2 = \begin{cases} \left[|x_q^I K_C + x_q^Q K_D - \hat{x}_q^I K_C - \hat{x}_q^Q K_D|^2 \right. \\ \left. +|x_q^I K_D - x_q^Q K_C - \hat{x}_q^I K_D + \hat{x}_q^Q K_C|^2\right]/2 & (i = \hat{i}) \\ \left[|x_q^I K_C + x_q^Q K_D|^2 + |\hat{x}_q^I K_C + \hat{x}_q^Q K_D|^2 \right. \\ \left. +|x_q^I K_D - x_q^Q K_C|^2 + |\hat{x}_q^I K_D - \hat{x}_q^Q K_C|^2\right]/2 & (i \neq \hat{i}). \end{cases}$$

An exact closed-form expression of the APEP can be calculated by using (13) and (14) from

$$\overline{\mathrm{PEP}}_{op} = \frac{1}{\pi}\int_0^{\frac{\pi}{2}} M_\gamma\left(-\frac{E_u}{4\sigma_n^2\left(1-\varrho^2\right)\sin^2\theta}\right)d\theta. \quad (15)$$

It is possible to have an easier form of this expression by upper bounding the error probability in (15) considering the maximum value of $\sin^2\theta = 1$ as follows [11, p. 230]

$$\overline{\mathrm{PEP}}_{op} \approx \frac{1}{2} M_\gamma\left(-\frac{E_u}{4\sigma_n^2\left(1-\varrho^2\right)}\right). \quad (16)$$

Assuming high signal-to-noise ratio (*SNR*), an asymptotic approximation can also be derived for $\overline{\mathrm{PEP}}_{op}$ with the aim of expressing the error probability in a simpler form to get useful insights for the key parameters

$$\overline{\mathrm{PEP}}_{op} \approx \frac{1}{2}\left(\frac{E_u\lambda_1}{2\sigma_n^2\sqrt{1-\varrho^2}}\right)^{-N_r} \approx \frac{1}{2}\left(\frac{2\sigma_n^2|\cos\beta_r|}{E_u\lambda_1}\right)^{N_r} \quad (17)$$

It is clear from (17) that $\overline{\mathrm{PEP}}_{op}$ depends on phase imbalance, variance of the noise, energy of the transmitted signal, estimation accuracy at Rx (λ_1) and the number of Rx antennas. In contrasting fashion, two remarkable points are proven with (17). First, the proposed optimal design is coherent to amplitude imbalance, i.e., $\overline{\mathrm{PEP}}_{op}$ does not dependent on ξ_r. Next, the diversity gain that can be calculated from (18) is equal to the number of Rx antennas (P_e is the probability of error) as

$$d = -\lim_{SNR\to\infty}\frac{\log P_e}{\log SNR}. \quad (18)$$

B. Non-Optimal ML Detector

A non-optimal detector is designed by assuming that $\boldsymbol{\chi}_p$, which is under the effect of IQI, has been sent and the traditional ML Rx that ignores IQI is used at the Rx side. In this case, supposing that K_1 and K_2 are unknown, the non-optimal detector is derived by ($\hat{q}$ is detected symbol index)

$$[\hat{i}, \hat{q}] = \arg\min_{i,q}\|\boldsymbol{y} - \sqrt{E_u}\boldsymbol{h}_i x_q\|^2. \quad (19)$$

The conditional PEP for the non-optimal case can be calculated by utilizing the following decision rule

$$\mathrm{PEP}_{no} = \Pr\left\{\|\boldsymbol{y} - \sqrt{E_u}\boldsymbol{h}_i x_q\|^2 > \|\boldsymbol{y} - \sqrt{E_u}\hat{\boldsymbol{h}}_i\hat{x}_q\|^2\right\}. \quad (20)$$

The non-optimal conditional PEP can also be written in Q-function as given in (21). This expression provides a rough analysis with approximated results and enables to observe the impacts of amplitude imbalance, i.e., (21) changes with ξ_r. However, as it is quite difficult to derive a PDF for (21), $\overline{\mathrm{PEP}}_{no}$ is calculated numerically by averaging the PEP_{no} values over a large number of channel realizations.

C. Average Bit Error Probability

Average bit error probability (ABEP) of the SM scheme can be upper bounded by the following well-known tight union bound technique [12]

$$\overline{\mathrm{BEP}}_b \leq \frac{1}{2^m}\sum_{i=1}^{2^m}\sum_{k=1}^{2^m}\frac{\overline{\mathrm{PEP}}_b B_{i,k}}{m}, \quad (22)$$

where $b \in \{op, no\}$ and $B_{i,k}$ is the number of bit errors relevant to the corresponding pairwise error event.

D. Complexity Analysis

The computational complexity is calculated as the number of real multiplications needed by any algorithm [13]. This number of multiplications to search through the all possibilities and evaluate the Euclidean distances, is computed as $C_{op} = 2^m(11N_r + 10) + 3$ for the optimal detector given in (10), while it is equal to $C_{no} = 8N_r 2^m$ for the non-optimal detector of (19). It means that the complexity of the proposed optimal

$$\mathrm{PEP}_{op} = Q\left(\sqrt{\frac{E_u}{2\sigma_n^2\left(1-\varrho^2\right)}\left(\|\boldsymbol{\chi}_p^I - \hat{\boldsymbol{\chi}}_p^I\|^2 + \frac{\|\boldsymbol{\chi}_p^Q - \hat{\boldsymbol{\chi}}_p^Q\|^2}{\xi_r^2} - \frac{2\varrho\left(\boldsymbol{\chi}_p^I - \hat{\boldsymbol{\chi}}_p^I\right)^T(\boldsymbol{\chi}_p^Q - \hat{\boldsymbol{\chi}}_p^Q)}{|\xi_r|}\right)}\right) = Q\left(\sqrt{\frac{E_u\gamma}{2\sigma_n^2(1-\varrho^2)}}\right). \quad (12)$$

$$\mathrm{PEP}_{no} = Q\left(\sqrt{\frac{E_u\left(\|\boldsymbol{\chi}_p - \hat{\boldsymbol{h}}_i\hat{x}_q\|^2 - \|\boldsymbol{\chi}_p - \boldsymbol{h}_i x_q\|^2\right)^2}{2\sigma_n^2\left(\|\hat{\boldsymbol{h}}_i^I\hat{x}_q^I - \boldsymbol{h}_i^I x_q^I\|^2 + \xi_r^2\|\hat{\boldsymbol{h}}_i^Q\hat{x}_q^Q - \boldsymbol{h}_i^Q x_q^Q\|^2 - 2\xi_r\sin\beta_r(\hat{\boldsymbol{h}}_i^I\hat{x}_q^I - \boldsymbol{h}_i^I x_q^I)^T(\hat{\boldsymbol{h}}_i^Q\hat{x}_q^Q - \boldsymbol{h}_i^Q x_q^Q)\right)}}\right) \quad (21)$$

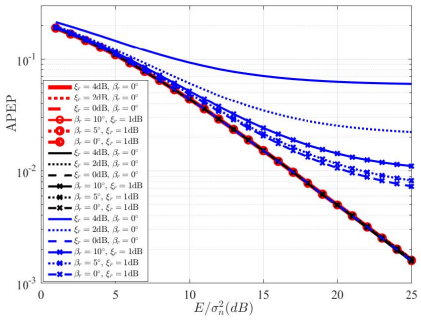

Fig. 2. APEP performance of the 2×1 SM-MIMO systems: red and blue curves represent simulation results of the optimal and non-optimal detectors, respectively, black curves represent analytical results of the optimal detector.

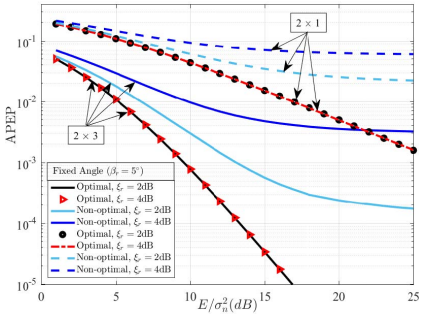

Fig. 3. APEP performance of the optimal and non-optimal receivers for 2×1 and 2×3 SM-MIMO systems for variable ξ_r and fixed β_r.

Rx is higher than that of the non-optimal one depending on the N_r at the same SE. In [13], complexity was also calculated as $8N_r 2^m$ for the perfect SM-MIMO transceiver. Hence, it can be concluded that the optimal ML detector has to deal with extra calculation burden to make SM robust against the IQI effect.

IV. Numerical Analysis and Results

The effects of amplitude and phase mismatches (ξ_r and β_r) beside the effect of diversity gain on the SM system performance are evaluated by computer simulations and analytical derivations. 2×1 and 2×3 SM-MIMO configurations are considered in this study and 4-QAM is utilized in both systems.

The results for the 2×1 SM system while fixing the amplitude mismatch to 1 dB and varying the phase imbalance among 0°, 5° and 10° are given in Fig. 2. The same system is also analyzed by fixing the phase imbalance to 0° while varying amplitude mismatch value between 0 dB, 2 dB and 4 dB and the obtained results are given in the same figure. It is observed that increasing IQI causes perceptible performance degradation on SM-MIMO system for the non-optimal Rx and amplitude IQI has more severe impacts than the phase IQI. Additionally, the error floor appears at slightly higher SNR values with the non-optimal Rx. The similar error floor is also observed in [8, Figs. 2–4]. In [8], although it is a part of the incoming signal, the term $K_2\sqrt{E_s}\mathbf{H}^* x^*$ of (7) was treated as additional noise. Hence, this approach does not provide a realistic solution. This issue is rectified in the non-optimal design, but an error floor is still observed.

As one of the outstanding points of this study, the optimal Rx design prevents the error floor. A decrease in APEP is observed even in high SNR values according to Fig. 2. For instance, more than 8 dB performance gain is achieved by using the optimal detector, while $\beta_r = 10^\circ$ and $\xi_r = 1$ dB. As another main advantage, the optimal design decreases the impairment of phase mismatch to the minimum and provides an amplitude IQI coherent system. Analytical results are perfectly matched with the computer simulation results. Moreover, it is worth mentioning that these improvements are achieved notwithstanding the additional complexity cost.

In Fig. 3, the results of 2×1 and 2×3 systems are compared while fixing β_r to 5° and setting ξ_r as 2 dB and 4 dB. It is clear that increasing the number of Rx antennas, due to the increasing diversity order, results in a remarkable system performance enhancement for the optimal Rx. For instance, the 2×3 SM-MIMO system has approximately 12 dB gain compared to the 2×1 setup at an APEP of 10^{-2}. Although the diversity gain of the system also increases with the non-optimal Rx, it is not as effective as the optimal case. Amplitude imbalance coherence of our optimal design, which is proven with (17), is also seen in Fig. 3, i.e., the APEP is the same for ξ_r= 2 dB and ξ_r= 4 dB for the optimal case.

V. Conclusion

In this study, the performance of the SM-MIMO scheme over Rayleigh fading channel has been analyzed in the presence of IQI. An optimal detector has been designed and compared with the non-optimal one. A tight upper bounded ABEP expression has been derived. Simulation results have shown that both amplitude and phase mismatches have severe degradation effect on SM-MIMO structure and should be carefully considered in future wireless communication systems. The optimal design outperforms the non-optimal one although having higher complexity. Our Rx designs are suitable to use for any channel configurations and M-ary modulation schemes.

References

[1] A. Gupta and E. R. K. Jha, "A survey of 5G network: Architecture and emerging technologies," *IEEE Access*, vol. 3, pp. 1206–1232, Jul. 2015.
[2] T. Schenk, *RF Imperfections in High-Rate Wireless Systems: Impact and Digital Compensation*, 1st ed. Springer, 2008.
[3] A.-A. A. Boulogeorgos, V. M. Kapinas, R. Schober, and G. K. Karagiannidis, "I/Q-imbalance self-interference coordination," *IEEE Trans. Wireless Commun.*, vol. 15, no. 6, pp. 4157–4170, Jun. 2016.
[4] Y. Tsai *et al.*, "Blind frequency-dependent I/Q imbalance compensation for direct-conversion receivers," *IEEE Trans. Wireless Commun.*, vol. 9, no. 6, pp. 1976–1986, Jun. 2010.
[5] R. Y. Mesleh *et al.*, "Spatial modulation," *IEEE Trans. Veh. Technol.*, vol. 57, no. 4, pp. 2228–2241, Jul. 2008.
[6] E. Basar *et al.*, "Index modulation techniques for next-generation wireless networks," *IEEE Access*, vol. 5, pp. 16693–16746, Aug. 2017.
[7] M. Di Renzo, H. Haas, A. Ghrayeb, S. Sugiura, and L. Hanzo, "Spatial modulation for generalized MIMO: Challenges, opportunities, and implementation," *Proc. IEEE*, vol. 102, no. 1, pp. 56–103, Jan. 2014.
[8] R. Mesleh *et al.*, "Impact of IQ imbalance on the performance of QSM multiple-input–multiple-output system," *IET Commun.*, vol. 10, no. 17, pp. 2391–2395, Nov. 2016.
[9] A. G. Helmy *et al.*, "On the robustness of spatial modulation to I/Q imbalance," *IEEE Commun. Lett.*, vol. 21, no. 7, pp. 1485–1488, Jul. 2017.
[10] A. Gouissem *et al.*, "Outage performance of cooperative systems under IQ imbalance," *IEEE Trans. Commun.*, vol. 62, no. 5, pp. 1480–1489, May 2014.
[11] M. K. Simon and M.-S. Alouini, *Digital Communication Over Fading Channels*, 2nd ed. Hoboken, NJ, USA: Wiley, 2004.
[12] E. Basar *et al.*, "Performance of spatial modulation in the presence of channel estimation errors," *IEEE Commun. Lett.*, vol. 16, no. 2, pp. 176–179, Feb. 2012.
[13] A. Younis, *Spatial Modulation: Theory to Practice*. Edinburgh, U.K.: Univ. Edinburgh, 2014. [Online]. Available: https://books.google.ca/books?id=JIvcoQEACAAJs